Materials Advances

ROYAL SOCIETY OF CHEMISTRY

PAPER

View Article Online
View Journal | View Issue

Check for updates

Cite this: *Mater. Adv.*, 2026, 7, 1443

4D printing of unaligned LCE: a facile approach to print photo mobile polymers

Domenico Sagnelli,*[a] Amalia D'Avino,†[a] Bryan Guilcapi,†[a] Tommaso Fasolino,[b] Anna De Girolamo Del Mauro,[b] Fausta Loffredo,[b] Fulvia Villani,[b] Giuseppe Nenna*[b] and Lucia Petti*[a]

Received 1st December 2025,
Accepted 18th December 2025

DOI: 10.1039/d5ma01396h

rsc.li/materials-advances

Here, we present a novel materials-based strategy that bypasses alignment procedures by integrating ZnO nanoparticles into an LCE ink, enabling a simplified, direct-write 4D printing process. We first demonstrate that ZnO doping significantly enhances the photo-actuation of non-aligned, injected LCE films, confirming the viability of the approach. Applying this strategy, we successfully printed reproducible actuators that exhibit large-amplitude bending and high actuation speeds, with performance comparable to traditionally aligned LCEs. The mechanism behind this enhancement is a synergistic photo-thermal effect; the ZnO nanoparticles increase light absorption *via* scattering while also dramatically improving the thermal diffusivity of the polymer matrix, leading to a more efficient and rapid mechanical response. By shifting the complexity from the manufacturing process to the material itself, this work offers a scalable pathway towards the rapid fabrication of complex, stimuli-responsive architectures for applications in soft robotics and adaptive systems.

Open Access Article. Published on 18 dicembre 2025. Downloaded on 11/05/2026 20:20:20.
This article is licensed under a Creative Commons Attribution-NonCommercial 3.0 Unported Licence.

1. Introduction

Additive manufacturing (AM), or 3D printing, has revolutionized the fabrication of complex structures, enabling rapid prototyping, design flexibility, and product customization across industries from aerospace to medicine.[1–6] A recent evolution of this technology is 4D printing, which incorporates "smart" materials capable of changing their shape or function over time in response to external stimuli such as heat, light, or electricity.[2–4,7] 4D printing is an innovative method in additive manufacturing that enables static objects to transform dynamically by the application of smart materials and subsequent exposure to varying stimuli, including temperature, light, and electricity.[8–11] The fourth dimension in 4D printing denotes the temporal alteration undergone by the component, making it programmable. This additional dimension signifies a predictable and intended transformation of the printed object over time, contingent upon three-dimensional space. This three-dimensional space is the precise configuration of voxels (x, y, and z coordinates) defined by mathematical principles and actualized by printing.[12,13]

Among the most promising candidates for 4D printing are liquid crystal elastomers (LCEs), which can undergo large, reversible deformations.[14–16] Photo-responsive LCEs, typically incorporating azobenzene moieties, are particularly attractive as they allow for precise, non-contact spatial and temporal control of actuation.[17] However, a significant bottleneck has hindered their widespread adoption in 4D printing: the need for macroscopic molecular alignment.[1,18] Traditionally, achieving high-performance actuation in LCEs has relied on complex, often slow, and equipment-intensive secondary processing steps to pre-align the liquid crystal director, such as mechanical rubbing of substrate surfaces, or the application of strong magnetic or electric fields.[14,18,19] While direct-write printing can impart a degree of shear-induced alignment, it hits fundamental limitations bound to the intrinsic dependance of liquid crystals (LC) to their transition temperatures. When the nematic–isotropic transition temperature (T_{NI}) is higher than the temperature reached during the printing process, mesogenic alignment can still be achieved.[20] In fact, if the printing speed is sufficiently low, the induced orientation can be preserved during the rapid UV polymerization. Conversely, when the processing temperature exceeds T_{NI}, obtaining aligned structures in the nozzle while the LCs are in isotropic temperature becomes challenging, is very likely to have random molecular orientation.[21–23]

In fact, in this regime, the material flows as a nearly Newtonian melt, so the Ericksen–Leslie flow-alignment mechanism is effectively switched off, and any transient orientation generated in the nozzle relaxes on timescales much shorter than the

[a] *Institute of Applied Sciences and Intelligent Systems of CNR, Pozzuoli 80072, Italy. E-mail: domenico.sagnelli@isasi.cnr.it, lucia.petti@cnr.it*
[b] *Energy and Sustainable Economic Development, ENEA, Italian National Agency for New Technologies, Portici Research Centre, Portici, Naples 80055, Italy. E-mail: giuseppe.nenna@enea.it*
† The authors contributed equally to the work.

© 2026 The Author(s). Published by the Royal Society of Chemistry

Open Access Article. Published on 18 diciembre 2025. Downloaded on 11/05/2026 20:20:20.
This article is licensed under a Creative Commons Attribution-NonCommercial 3.0 Unported Licence.

residence time. As a result, printing liquid crystal mixtures with high melting temperature with $T_{NI} < T$ predominantly produces isotropic or weakly paranematic strands, unless an external field or surface anchoring is introduced during or immediately after deposition.[24]

Recent temperature-responsive LCE DIW studies instead maintain the ink slightly below or around T_{NI} (for example, printing near 60–65 °C for $T_{NI} \approx 63$ °C[25]), specifically to exploit the nematic rheology and obtain strong shear-induced alignment and monodomain filaments. Various work of literature deliberately prints near T_{NI} and/or at a slow speed to facilitate the isotropic to nematic transition.[7] In contrast, more restrictive scenarios with printing temperature significantly higher than T_{NI} show is easier extrusion (low viscosity, stable flow), but the fundamental loss of nematic order during printing makes it significantly more difficult to program well-defined director architectures compared to the literature strategies.

To address the constraints imposed by the T_{NI} and to minimize reliance on surface-induced alignment, we introduce a materials-driven strategy that eliminates the need for thermal stabilization prior to curing, allowing immediate photopolymerization during deposition. Our working hypothesis is that incorporating ZnO nanoparticles into the LCE formulation will (i) shorten the transition interval between Tm and T_{NI} and (ii) amplify the intrinsic photothermal response of the material. This dual effect is expected to compensate for the absence of long-range pre-alignment and to enable a streamlined, direct-write 4D-printing workflow for the fabrication of functional light-responsive actuators. This theory can fill an important gap: by allowing a simplified printing process, reducing thermal equilibration times, and improving the feasibility of intelligent photothermal actuators.

In this work, we validate this hypothesis through a two-stage investigation. First, we establish the foundational effect of ZnO doping in non-aligned, standard LCE films to isolate its impact on photo-actuation. Subsequently, we apply this optimized material to an extrusion-based 4D printing process, demonstrating the fabrication of reproducible, high-performance actuators without any secondary alignment process. Finally, we elucidate the underlying mechanism, showing that the performance enhancement is driven by a synergy of improved light absorption and a dramatic increase in thermal diffusivity, which facilitates a more rapid and efficient photo-mechanical response.

2. Materials & methods

2.1. Materials

LC monomers 4-methoxybenzoic acid 4-(6-acryloyloxyhexyloxy)-phenyl ester (MAPE), 4[4[6-acryloxyhex-1-yl]oxyphenyl]carboxybenzonitrile (AOCB), 1,4-Bis-[4-(6-acryloyloxyhexyloxy)benzoyloxy]-2-methylbenzene (AOBM), 4,4′-bis[9-(acryloyloxy)nonyloxy]azobenzene (A9ZA9) were purchased at synthon chemicals (Germany), and the photoinitiator bis(2,4,6-trimethylbenzoyl)-phenylphosphineoxide from Sigma Aldrich. Elvamide was provided by Beamco. Other chemicals were provided by Sigma-Aldrich.

2.2. Methods

2.2.1. Preparation of the cell reactor. Photo-actuator synthesis cells were prepared using glass slides and plastic spacers. The method used was previously discussed in literature with some differences.[19,26,27] In particular the cells were or not rubbed/coated in function of the sample needed.

2.2.2. Synthesis of the photo-mobile polymer films. The PMP and PMP/ZnO films were prepared following a protocol described elsewhere.[27] In brief, the reaction mixture was dissolved in dichloromethane and heated up at 70 °C until all solvent was removed. Then, the reaction mixture was left to recrystallize at room temperature overnight. The reaction cell was heated to 95 °C and the mixture infiltrated by capillarity. After the infiltration, the sample was moved on a second hotplate set at the nematic temperature (50 °C) and photopolymerized for 1 h (30 minutes each side) using a UV lamp emitting at 405 nm (12 mW cm^{-2}) and successively left for 24 hours at 50 °C. Nanoparticles dimension was 100 nm.

2.2.3. Printing equipment. A Hyrel3D system 30 M printer, including a KR2 printhead and low-volume HTK print cartridges, was utilized for all 3D printing activities. The ink was introduced into the print head, the head heated at isotropic temperature (90 °C), the plunger was advanced until the ink appeared at the tip, and the print head was maintained upright for over 30 minutes to eliminate any air bubbles. The system was permitted to cool to ambient temperature prior to the attachment of the 400 μm diameter nozzle to the print head. The LC mix was deposited on a heated bed (50 °C), utilizing a print speed of 20 mm s^{-1}, a layer height of 50 μm, and a linewidth of 400 μm. During the printing process, UV light (405 nm) was utilized to polymerize the deposited mixture.

The ink used in the printer was the same used in micro-cell reactors.

2.2.4. Characterization of LCEs. The motion characteristics of PMP films, including its angular position and bending velocity, were examined by capturing video frames subsequent to the stimulation with the light beam. All experiments presented were repeated a minimum of three times to ensure the trends are robust and reproducible. Lasers with wavelengths of 457 and 405 nm were used as light source, meticulously positioning the light beam on the surface of the PMP film. Each frame was obtained *via* an experimental process lasting (N) seconds, utilizing a high-resolution camera (General Web Cam HD 1980 × 1020) that captured a frame every 0.25/0.5 seconds. The system consists of an automated gate operated by a servo motor controlled by Arduino, which opens one second after the experiment starts and closes at (N/2 + 1) seconds post-opening, enabling observation of the PMP behavior in both regimes laser light on and off while the system continues data acquisition. The entire process was conducted using a bespoke MathWorks MATLAB code for control-acquisition data and angular data reconstruction. The software is available on github (https://github.com/BryanGuilcapi/Acquisition_Data_Pictures).

© 2026 The Author(s). Published by the Royal Society of Chemistry

Open Access Article. Published on 18 dicembre 2025. Downloaded on 11/05/2026 20:20:20.
This article is licensed under a Creative Commons Attribution-NonCommercial 3.0 Unported Licence.

The experimental configuration is illustrated in SI, Fig. S2.

2.2.5. Thermographic measurements. The thermal measurements were performed using a FLIR camera (FLIR A-50). The samples were irradiated with a laser at a wavelength of 457 nm; the laser spot was widened using a beam expander (Thorlabs EL-25-10x-A) to irradiate the whole sample. The laser output was calibrated after the beam expander to find out the density in mW cm^{-2} that would impinge the sample. The experiments were performed as a sweep in function of laser power that varied from 0 to 4 mW cm^{-2}.

The data analysis was performed using the science SDK provided by FLIR. The SDK was used by interfacing it with Matlab. The software is available on github with a simple guide, (https://github.com/Docdomee/FLIR_SDK/).

3. Results & discussion

3.1. Establishing the principal effect of ZnO on LCE photo-responsivity in the absence of mechanical alignment

In our previous work, we showed that incorporating ZnO nanoparticles enhances the photo-mechanical response of aligned liquid crystal elastomers (LCEs), where molecular order is induced by surface rubbing.[27] These results established ZnO as a performance-enhancing additive. A critical question remained, however: is this nanoparticle-induced enhancement strong enough to be effective in the complete absence of complex, and often laborious, pre-alignment procedures?

To answer this question, we first designed an experiment to isolate the effect of ZnO. We fabricated LCE films diffusing the monomers within glass mini-reactors without any external alignment techniques. Specifically, we prepared two types of non-aligned cells: one set lacked any surface coating and mechanical rubbing (*_NC series), while another was coated with elvamide polymer but still lacked the crucial rubbing step (*_NR series).

The results presented in Fig. 1 clearly show the impact of the nanoparticles on the photo-mobile polymer (PMP) film. In a direct comparison, the ZnO-doped films (ZnO06%_NC and ZnO06%_NR) exhibited a dramatically improved bending angle and actuation speed compared to the pristine LCE control sample (C_NR), which showed minimal response. This initial finding confirms that ZnO doping can effectively compensate for the lack of a pre-defined molecular director (Fig. 1).

Building upon this, we conducted a more systematic investigation by varying the ZnO concentration (0, 1.5, 3, and 6 wt%) and the wavelength of the light stimulus (457 nm and 405 nm), as shown in Fig. 2. The results reveal a coupled relationship between nanoparticle concentration and stimulus wavelength. At higher concentrations (3 and 6 wt%), a clear and consistent performance enhancement was observed regardless of the wavelength (Fig. 2).

However, the behaviour at the lower concentration of 1.5 wt% was strongly wavelength-dependent. When stimulated with 405 nm light, the 1.5% ZnO sample showed a significant improvement in actuation (Fig. 2(e)) especially at lower power density reaching a plateau, reflecting an overall behaviour. Conversely, under 457 nm light, its performance was lower than the pristine control (Fig. 2(d)). This observation is consistent with our findings on traditionally rubbed cells,[28] where 1.5% ZnO doping instead resulted in actuation comparable to the control. In this case, in absence of external alignment 1.5% ZnO limits the ability of the material to respond to light possibly because the lesser interaction with LCs and lower ability of azobenzene moieties to efficiently actuate with a light at 457 nm. This is probably due to the different optical properties of azobenzene moieties at the different wavelength radiation, consequently using less effective wavelength we would need more doping agent.

These data suggest that while higher ZnO concentrations provide a robust, global enhancement, the benefit of lower concentrations becomes evident only under more favourable stimulation conditions (*i.e.*, 405 nm) in systems with no pre-alignment. We hypothesize that higher concentrations ($\geq$3 wt%) are required to form a more densely packed nanoparticle network, which ensures efficient energy transfer

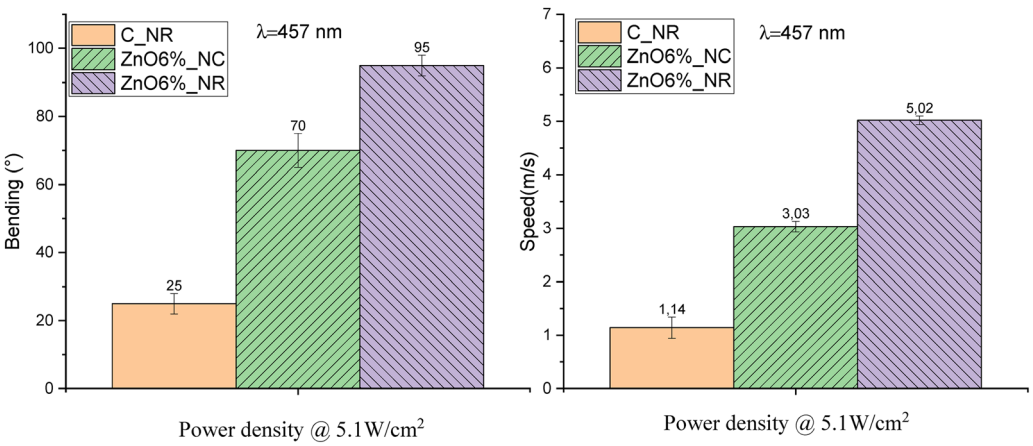

Fig. 1 (a) Bending and (b) speed of PMP and PMP/ZnO prepared without rubbing (ZnO6%_NR; C_NR) or elvamide coating (ZnO6%_NC_457). The measurements were carried out with 457 nm laser.

Open Access Article. Published on 18 dicembre 2025. Downloaded on 11/05/2026 20:20:20.
This article is licensed under a Creative Commons Attribution-NonCommercial 3.0 Unported Licence.

throughout the polymer matrix under all conditions. Nevertheless, these results unequivocally confirm that ZnO doping is a viable materials-based strategy for enhancing photo-responsivity, providing a strong rationale for its application in a simplified 4D printing process.

3.2. Application of the ZnO-doping strategy to simplify the 4D printing of photo-actuators

Using the standard films' foundation results, we used ZnO-doping in a direct-write 4D printing process. It is well-established that in extrusion-based printing, a degree of shear-induced molecular alignment is naturally imparted to the material as it passes through the nozzle. Our central objective was to investigate if the synergistic effect between this inherent, partial alignment and the ZnO-induced enhancement was sufficient to create high-performance actuators without any post-extrusion induced alignment and not wait-time for the nematic organization to happen. Furthermore, the materials would be polymerized *in situ* while being extruded.

Using an ink with the same composition as our base materials, we successfully printed simple geometries, such as cantilevers, at a rapid rate (20 mm s^{-1}) with *in situ* UV polymerization, eliminating the need for post-processing steps (Fig. 3). The printed cantilevers doped with ZnO exhibited a large and rapid photo-actuation, including the ability to enter a high-speed self-vibration mode under continuous irradiation

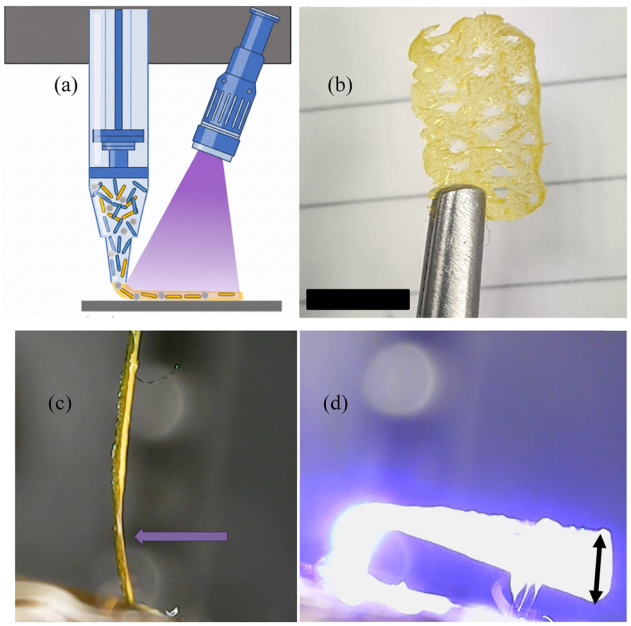

Fig. 3 (a) Set-up used to print and polymerize the mixtures of LCs. (b) 3D printed mesh without ZnO, scale bar represents 1 cm; (c), (d) 3D printed film before and during the actuation with 405 nm laser where the LCEs film doped with ZnO bends and start self-vibration at high speed. The purple arrow in Fig. 4(c) represent the impinging light the black arrow in Fig. 4(d) represents the vibration span of the material (3 mm).

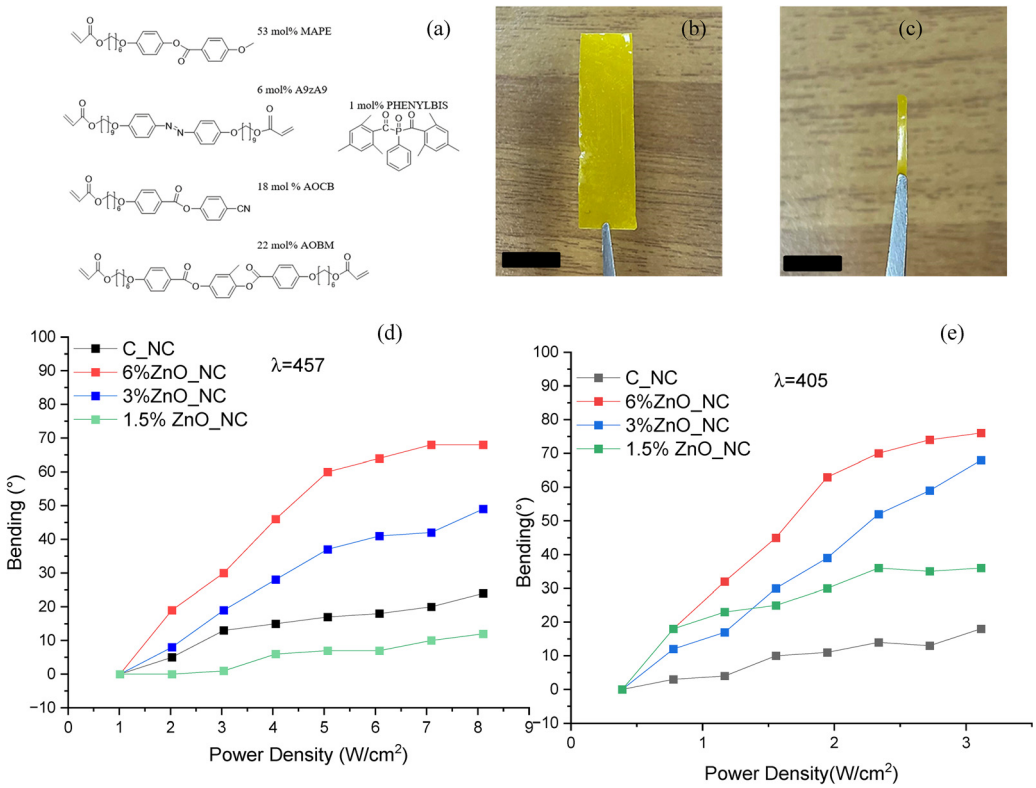

Fig. 2 (a) Structures and molar concentration of the LC monomers used to prepare the pristine PMP and PMP/ZnO composites (b) and (c) images[28] of liquid crystal polymer films doped with ZnO, the scalebar represents 1 cm. (d) Bending of doped PMPs when irradiated with a laser light at 457 nm and (e) 405 nm.

© 2026 The Author(s). Published by the Royal Society of Chemistry

Open Access Article. Published on 18 dicembre 2025. Downloaded on 11/05/2026 20:20:20.
This article is licensed under a Creative Commons Attribution-NonCommercial 3.0 Unported Licence.

(Fig. 3(d)). In contrast, control samples printed without ZnO showed no appreciable movement under the same conditions (Fig. 3(b)). Crucially, the actuators bend towards the light source (Fig. 3(c)) and goes back to start position, a hallmark of the contractile phase transition driven by the azobenzene moieties on the illuminated surface. This directional contraction is fundamentally different from a simple, non-directional thermal expansion effect that might occur in any polymer. While the process is amplified by the ZnO-enhanced photothermal effect, the actuation itself is contingent on the presence of the photo-switchable azobenzene. Indeed, as we have previously established, control samples fabricated with ZnO but lacking the azobenzene component show no photo-induced movement under illumination, confirming that the observed mechanical work is generated by the LCE's intrinsic photo-mechanical properties and not by simple heating.[27]

To evaluate the homogeneity and repeatability of the process across different printing directions, a planar 'sun-like' geometry was designed and printed (Fig. 4(d)). The individual arms were analyzed, and the results demonstrated excellent reproducibility. All tested arms exhibited similar, high-performance actuation, reaching a maximum bending of up to 100 degrees, irrespective of their original printing orientation (Fig. 4(a)). The performance of these printed actuators was superior to the non-aligned cast films (Fig. 1 and 2) and was comparable to that of traditionally aligned samples doped with ZnO, validating our simplified printing approach (SI, Fig. S1). Furthermore, the actuation speed showed a clear and tunable dependence on the incident laser power density (Fig. 4(b) and (c)), highlighting the controllability of the printed structures. A closer look at the instantaneous velocity (Fig. 4(c)) reveals that upon illumination, the speed rapidly peaks within the first 2–3 seconds and then decreases as the arm approaches its maximum bending angle. Notably, this peak occurs earlier at higher power densities, suggesting the intervention of more rapidly activated thermal phenomena that will be discussed in the next section.

3.3. Unveiling the mechanism: a synergy of enhanced light absorption and thermal transport

To explain the performance boost in ZnO-doped printed actuators, we looked at their microscopic structure and photothermal properties. To see if the improved performance was due to a more organized molecular structure, we used polarized optical microscopy (POM) (SI, Fig. S3) to analyze the printed films. The POM analysis confirms that the printed ZnO-doped material lacks the large-scale, uniform birefringent domains characteristic of LCEs prepared with traditional rubbing methods (SI, Fig. S4). This observation is critical: it demonstrates

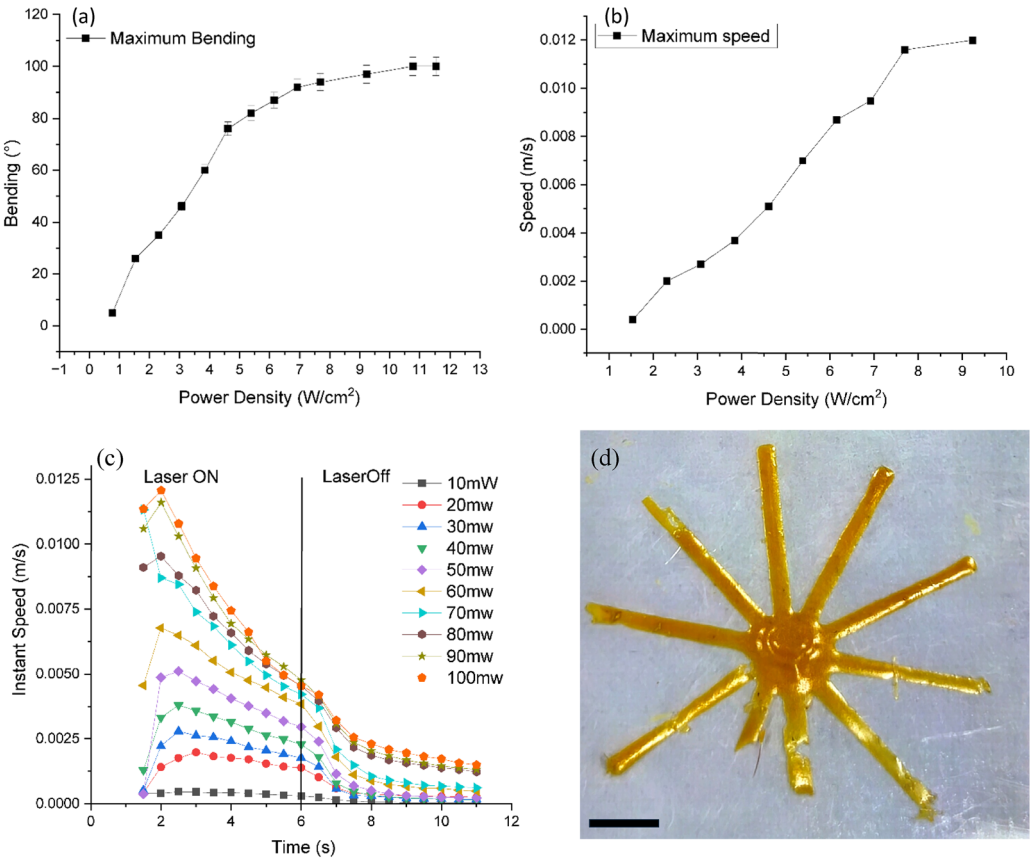

Fig. 4 (a) Maximum average bending and. (b) maximum average speed of 3d printed sun-arms (c) Instant speed per frame of materials (0.5 s) at various laser powers. (d) Photo of a sun-like 3d printed material, scale bar 1 cm. The picture of the sun-like print shows the print after some arms were cut off for testing.

Open Access Article. Published on 18 diciembre 2025. Downloaded on 11/05/2026 20:20:20.
This article is licensed under a Creative Commons Attribution-NonCommercial 3.0 Unported Licence.

that the superior actuation is not attributable to the formation of a macroscopic, highly ordered nematic structure. Any residual micro-alignment, if present, would be minimal and not the driving factor for the strong photo-actuation observed, which aligns with the actual thermographic and mechanical data.

The ZnO nanoparticles (100 nm) may impose anchoring conditions on the nematic director field, leading to local distortions when their size and concentration exceed critical thresholds.[29,30] Specifically, when the nanoparticle size surpasses the surface extrapolation length, strong distortions and topological defects form around the particles, reducing the overall nematic order parameter.[29,30] Moreover, at concentrations such as 6%, these distortions accumulate and promote a phase crossover from a uniform nematic phase to a distorted or paranematic phase, effectively disrupting the nematic alignment. This behavior aligns with observations for other spherical nanoparticles, where increasing particle content beyond about 0.4% weight leads to a notable reduction in nematic order due to similar interfacial and elastic effects.[29,30]

Is instead clear in literature that small size—often a few nanometers—induce minimal elastic distortion in the liquid crystal director field.[19,31] Additionally, their metallic nature and the strong surface plasmon resonance effects enable enhanced photothermal and optical functionalities without significantly perturbing the nematic phase.[19,31] For instance, gold or silver nanoparticles embedded in liquid crystalline elastomers show efficient photo-actuation performance while preserving the local order.[19,31]

Our data point towards a synergistic mechanism rooted in the material's optical and thermal properties. As we have previously demonstrated, ZnO nanoparticles act as possible scattering centers within the polymer matrix.[27] This scattering may increases the optical path length of the incident light, effectively trapping it within the film and leading to a significant increase in the overall light absorption, particularly in the 400–500 nm wavelength range where the pristine LCE's absorbance begins to decrease. This enhanced absorption means that more of the light's energy is converted into heat within the material, but photo-thermal conversion is only part of the story. The key to the enhanced performance lies in how efficiently this generated heat affects the material properties. To investigate this, we measured the thermal properties of the printed films (Fig. 5). The thermographic measurements reveal a striking difference: the thermal diffusivity of the ZnO-doped material is approximately four times higher than that of the undoped control (Fig. 5(a)). This indicates a much more rapid and efficient diffusion of heat throughout the ZnO-doped polymer matrix. While the temperature recorded on the surface of the doped samples was lower at the plateau (Fig. 5(b)), suggesting a better heat diffusion and dissipation.

A clear mechanism emerges, the ZnO nanoparticles first enhance the absorption of light, generating more heat. Then, due to the improved thermal diffusivity, this heat is rapidly and uniformly distributed throughout the actuator's bulk. This leads to a faster, more efficient, and more homogeneous phase transition,[32] which is the ultimate driver of the mechanical

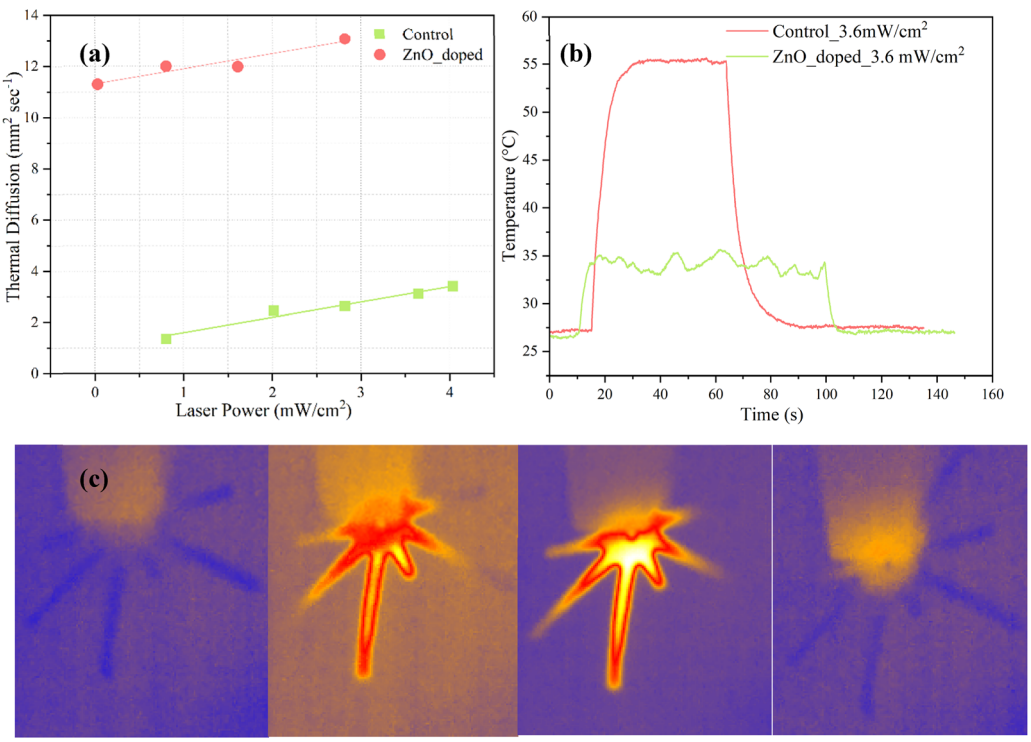

Fig. 5 (a) Thermal diffusivity of materials tested in function of the laser power density. (b) Temperature profile of control and doped materials showing that at the plateau the surface temperature is lower on ZnO doped material (c) frames of the IR video of a sample being irradiated.

© 2026 The Author(s). Published by the Royal Society of Chemistry

Open Access Article. Published on 18 dicembre 2025. Downloaded on 11/05/2026 20:20:20.
This article is licensed under a Creative Commons Attribution-NonCommercial 3.0 Unported Licence.

work. Therefore, the simplified 4D printing process is enabled by a materials-driven photo-thermal enhancement that effectively compensates for the lack of a macroscopic, pre-aligned molecular structure.

4. Conclusions

In this work, we have demonstrated a novel and facile materials-based strategy to overcome limitations in the 4D printing of liquid crystal elastomers. By integrating ZnO nanoparticles into an LCE ink, we have successfully fabricated high-performance photo-actuators using a simplified, direct-write process. Our findings show that ZnO doping is remarkably effective at enhancing photo-actuation even in the complete absence of traditional alignment methods, as confirmed by our initial studies on cast films. When applied to an extrusion-based 4D printing process, this material strategy, leveraging the synergy between shear-induced alignment and nanoparticle enhancement, yielded reproducible actuators with large-amplitude bending and high actuation speeds, performing on par with traditionally fabricated aligned LCEs.

Furthermore, we have elucidated the mechanism behind this performance enhancement. The superior actuation is not due to the formation of a macroscopic, ordered nematic structure, but rather to a synergistic photo-thermal effect. The ZnO nanoparticles serve a dual function: they increase light absorption *via* scattering and, crucially, they dramatically improve the thermal diffusivity of the polymer matrix. This allows for a more rapid and efficient conversion of light into the heat that drives the nematic-to-isotropic phase transition, resulting in a faster and stronger mechanical response.

In conclusion, this work presents a significant step towards making 4D-printed LCE systems more accessible and scalable. By shifting the complexity from the process (*e.g.*, external alignment fields, precise temperature control) to the material itself (*i.e.*, nanoparticle doping), we open the door to the rapid fabrication of complex, stimuli-responsive architectures. Future work will focus on optimizing nanoparticle concentration and dispersion, and exploring the printing of true three-dimensional geometries for applications in soft robotics, adaptive systems, and responsive packaging.

Author contributions

The manuscript was ideated and written by Domenico Sagnelli, the main experiments were performed by Domenico Sagnelli and Amalia D'avino. Bryan Guilcapi and Tommaso Fasolino were of support for the experimental work. The work was supported by fruitful advice and discussions by Anna De Girolamo Del Mauro, Fausta Loffredo and Fulvia Villani. The paper was revised by Lucia Petti and Giuseppe Nenna as coordinators of the activity, with the support of all the authors. All authors have given approval to the final version of the manuscript.

Conflicts of interest

There are no conflicts to declare.

Data availability

All data supporting the findings of this study are available within the paper and its supplementary information (SI) files. Supplementary information includes a video showing the printed material in action and more details on the printed material properties. See DOI: https://doi.org/10.1039/d5ma01396h.

To watch and analyze the thermographic raw data contact the corresponding author.

Acknowledgements

The authors gratefully acknowledge support for this work from the Proof-of-Concept project named ''ALICE-Actuators based on LIght sensitive CompositE'' funded by private investor Eureka! TT S.r.l. The authors acknowledge the Teledyne FLIR Customer Support for the precious assistance related to the FLIR Research Studio software and the A-50 management.

References

1 M. del Pozo, J. A. H. P. Sol, A. P. H. J. Schenning and M. G. Debije, 4D Printing of Liquid Crystals: What's Right for Me?, *Adv. Mater.*, 2022, **34**(3), 2104390, DOI: 10.1002/adma.202104390.
2 S. Li, M. Gao, W. Shi, X. Sun, Y. Zhou, L. Liu, J. Qiu, X. Gao, J. Sun, X. Liu and Z. Gu, Engineering Stimuli-Responsive Shape-Morphing through High-Resolution 4D Printing, *Responsive Mater.*, 2025, **3**(4), e70025, DOI: 10.1002/rpm2.70025.
3 S. Tibbits, 4D Printing: Multi-Material Shape Change, *Archit. Des.*, 2014, **84**(1), 116–121, DOI: 10.1002/ad.1710.
4 J. Sunte, A Review on 4D – Printing Design, *Materials*, 2022, 99–108.
5 Y. Liu and S. L. Sing, A Review of Advances in Additive Manufacturing and the Integration of High-Performance Polymers, Alloys, and Their Composites, *Mater. Sci. Addit. Manuf.*, 2023, **2**(3), 1587, DOI: 10.36922/msam.1587.
6 I. Karakurt and L. Lin, 3D Printing Technologies: Techniques, Materials, and Post-Processing, *Curr. Opin. Chem. Eng.*, 2020, **28**, 134–143, DOI: 10.1016/j.coche.2020.04.001.
7 G. Hu, B. Zhang, S. M. Kelly, J. Cui, K. Zhang, W. Hu, D. Min, S. Ding and W. Huang, Photopolymerisable Liquid Crystals for Additive Manufacturing, *Addit. Manuf.*, 2022, **55**, 102861, DOI: 10.1016/j.addma.2022.102861.
8 C. M. Yakacki, M. Saed, D. P. Nair, T. Gong, S. M. Reed and C. N. Bowman, Tailorable and Programmable Liquid-Crystalline Elastomers Using a Two-Stage Thiol-Acrylate Reaction, *RSC Adv.*, 2015, **5**(25), 18997–19001, DOI: 10.1039/c5ra01039j.

© 2026 The Author(s). Published by the Royal Society of Chemistry

Open Access Article. Published on 18 diciembre 2025. Downloaded on 11/05/2026 20:20:20. This article is licensed under a Creative Commons Attribution-NonCommercial 3.0 Unported Licence.

9 H. Wang and J. Guo, Recent Advances in 4D Printing Hydrogel for Biological Interfaces, *Int. J. Mater. Form.*, 2023, **16**(5), 55, DOI: 10.1007/s12289-023-01778-9.
10 J. F. Henriques, A. M. Sousa and A. P. Piedade, 4D Printing: Reality or Myth?, *4D Print.*, 2025, **1**(1), 5–38, DOI: 10.1108/4DP-12-2024-0002.
11 X. Kuang, D. J. Roach, J. Wu, C. M. Hamel, Z. Ding, T. Wang, M. L. Dunn and H. J. Qi, Advances in 4D Printing: Materials and Applications, *Adv. Funct. Mater.*, 2019, **29**(2), 1805290, DOI: 10.1002/adfm.201805290.
12 J.-J. Wu, L.-M. Huang, Q. Zhao and T. Xie, 4D Printing: History and Recent Progress, *Chin. J. Polym. Sci.*, 2018, **36**(5), 563–575, DOI: 10.1007/s10118-018-2089-8.
13 E. Pei, G. H. Loh and S. Nam, Concepts and Terminologies in 4D Printing, *Appl. Sci.*, 2020, **10**(13), 4443, DOI: 10.3390/app10134443.
14 T. Ikeda, J. I. Mamiya and Y. Yu, Photomechanics of Liquid-Crystalline Elastomers and Other Polymers, *Angew. Chem., Int. Ed.*, 2007, **46**(4), 506–528, DOI: 10.1002/anie.200602372.
15 L. T. de Haan, C. Sánchez-Somolinos, C. M. W. Bastiaansen, A. P. H. J. Schenning and D. J. Broer, Engineering of Complex Order and the Macroscopic Deformation of Liquid Crystal Polymer Networks, *Angew. Chem., Int. Ed.*, 2012, **124**(50), 12637–12640, DOI: 10.1002/ange.201205964.
16 G. Hu, B. Zhang, S. M. Kelly, J. Cui, K. Zhang, W. Hu, D. Min, S. Ding and W. Huang, Photopolymerisable Liquid Crystals for Additive Manufacturing, *Addit. Manuf.*, 2022, **55**, 102861, DOI: 10.1016/j.addma.2022.102861.
17 D. Sagnelli, A. D'Avino, M. Rippa, A. Vestri, V. Marchesano, G. Nenna, F. Villani, G. Ardila, S. Centi, F. Ratto and L. Petti, Photomobile Polymer–Piezoelectric Composite for Enhanced Actuation and Energy Generation, *ACS Appl. Opt. Mater.*, 2023, **1**(10), 1651–1660, DOI: 10.1021/acsaom.3c00227.
18 T. H. Ware, M. E. McConney, J. J. Wie, V. P. Tondiglia and T. J. White, Voxelated Liquid Crystal Elastomers, *Science*, 2015, **347**(6225), 982–984, DOI: 10.1126/science.1261019.
19 D. Sagnelli, A. D'Avino, M. Rippa, A. Vestri, V. Marchesano, G. Nenna, F. Villani, G. Ardila, S. Centi, F. Ratto and L. Petti, Photomobile Polymer–Piezoelectric Composite for Enhanced Actuation and Energy Generation, *ACS Appl. Opt. Mater.*, 2023, **1**(10), 1651–1660, DOI: 10.1021/acsaom.3c00227.
20 C. Zhang, X. Lu, G. Fei, Z. Wang, H. Xia and Y. Zhao, 4D Printing of a Liquid Crystal Elastomer with a Controllable Orientation Gradient, *ACS Appl. Mater. Interfaces*, 2019, **11**(47), 44774–44782, DOI: 10.1021/acsami.9b18037.
21 V. Borshch, Y.-K. Kim, J. Xiang, M. Gao, A. Jákli, V. P. Panov, J. K. Vij, C. T. Imrie, M. G. Tamba, G. H. Mehl and O. D. Lavrentovich, Nematic Twist-Bend Phase with Nanoscale Modulation of Molecular Orientation, *Nat. Commun.*, 2013, **4**(1), 2635, DOI: 10.1038/ncomms3635.
22 A. Ranjkesh, Z. Alipanah, S. Kiani, M. S. Zakerhamidi and T.-H. Yoon, A Method to Find the Initial Temperature Range of the Short-Range Order in the Isotropic Phase of Nematic Liquid Crystals Based on the Electro-Optical Kerr Effect, *J. Mol. Liq.*, 2019, **274**, 646–652, DOI: 10.1016/j.molliq.2018.11.028.
23 S. Dhara and N. V. Madhusudana, Enhancement of the Orientational Order Parameter of Nematic Liquid Crystals in Thin Cells, *Eur. Phys. J. E*, 2004, **13**(4), 401–408, DOI: 10.1140/epje/i2003-10084-8.
24 Y. Kawamura and S. Iwayanagi, Complex Shear Viscosity of Liquid Crystals in the Isotropic Phase of Nematics, *Mol. Cryst. Liq. Cryst.*, 1977, **38**(1), 239–249, DOI: 10.1080/15421407708084390.
25 S. Li, Z. Song, Y. Fan, D. Wei and Y. Liu, Four-Dimensional Printing of Temperature-Responsive Liquid Crystal Elastomers with Programmable Shape-Changing Behavior, *Biomimetics*, 2023, **8**(2), 196, DOI: 10.3390/biomimetics8020196.
26 D. Sagnelli, M. Rippa, A. D'Avino, A. Vestri, V. Marchesano and L. Petti, Development of LCEs with 100% Azobenzene Moieties: Thermo-Mechanical Phenomena and Behaviors, *Micromachines*, 2022, **13**, 1665, DOI: 10.3390/MI13101665.
27 D. Sagnelli, M. Calabrese, O. Kaczmarczyk, M. Rippa, A. Vestri, V. Marchesano, K. Kortsen, V. C. Crucitti, F. Villani, F. Loffredo, C. Borriello, G. Nenna, M. Cocca, V. Ambrogi, K. Matczyszyn, F. Simoni and L. Petti, Photo-Responsivity Improvement of Photo-Mobile Polymers Actuators Based on a Novel Lcs/Azobenzene Copolymer and Zno Nanoparticles Network, *Nanomaterials*, 2021, **11**(12), 3320, DOI: 10.3390/nano11123320.
28 A. D'Avino, D. Sagnelli, A. Vestri, M. Rippa, V. Marchesano, V. Ambrogi, A. De Girolamo, F. Loffredo, F. Villani, G. Nenna and L. Petti, Optimization of PMP Films' Production and Mechanical Properties Based on ZnO Nanoparticles Addition. SPIE 12584, Smart Mater, *Optoelectron. Lett.*, 2023, **12584**, 1258405, DOI: 10.1117/12.2665616.
29 C.-H. Chen and I. Dierking, Nanoparticles in Thermotropic and Lyotropic Liquid Crystals, *Front. Soft Matter*, 2025, **4**, DOI: 10.3389/frsfm.2024.1518796.
30 C. Kyrou, S. Kralj, M. Panagopoulou, Y. Raptis, G. Nounesis and I. Lelidis, Impact of Spherical Nanoparticles on Nematic Order Parameters, *Phys. Rev. E*, 2018, **97**(4), 042701, DOI: 10.1103/PhysRevE.97.042701.
31 J. Xu, S. Chen, W. Yang, B. Qin, X. Wang, Y. Wang, M. Cao, Y. Gao, C. Li and Y. Dong, Photo Actuation of Liquid Crystalline Elastomer Nanocomposites Incorporated with Gold Nanoparticles Based on Surface Plasmon Resonance, *Soft Matter*, 2019, **15**(30), 6116–6126, DOI: 10.1039/C9SM00984A.
32 J. Zhang, S. Liu, X. Wang, X. Zhang, X. Hu, L. Zhang, Q. Sun and X. Liu, 4D Printable Liquid Crystal Elastomers with Restricted Nanointerfacial Slippage for Long-Term-Cyclic-Stability Photothermal Actuation, *Mater. Horiz.*, 2024, **11**(10), 2483–2493, DOI: 10.1039/D3MH02230G.

© 2026 The Author(s). Published by the Royal Society of Chemistry